

Instability of a fluctuating biomimetic membrane driven by an applied uniform DC electric field

Zongxin Yu, Shuozhen Zhao, Michael J. Miksis, and Petia M. Vlahovska
Engineering Sciences and Applied Mathematics, Northwestern University

(Dated: Feb 13 2025)

The linear stability of a lipid membrane under a DC electric field, applied perpendicularly to the interface, is investigated in the electrokinetic framework, taking account to the dynamics of the Debye layers formed near the membrane. The perturbed charge in the Debye layer redistributes and destabilizes the membrane via electrical surface stress interior and exterior to the membrane. The instability is suppressed as the difference in the electrolyte concentration of the solutions separated by the membrane increases, due to a weakened base state electric field near the membrane. This result contrasts with the destabilizing effect predicted using the leaky dielectric model in cases of asymmetric conductivity. We attribute this difference to the varying assumptions about the perturbation amplitude relative to the Debye length, which result in different regimes of validity for the linear stability analysis within these two frameworks.

I. INTRODUCTION

Cells are enveloped by thin ion-impermeable membranes that isolate the cell interior from the environment. The response of biological membranes and cells to electric fields has received a lot of attention, due to practical applications in cell manipulation, such as fusion and electroporation [1, 2]. These processes rely on the controlled destabilization of membranes [3, 4], where electric fields influence membrane fluctuations, alter geometry through stretching and compression [5, 6], and modify mechanical properties such as tension and bending [7]. Despite extensive experimental [5, 6] and theoretical studies, the fundamental mechanisms governing membrane destabilization in electric fields remain an area of ongoing research. Theoretical models for instability analysis involve two main approaches: the leaky dielectric model (LDM) and the Poisson-Nernst-Planck (PNP) model.

The leaky dielectric model (LDM) assumes that free charge is confined to interfaces separating media with different electric properties (conductivity and permittivity), while the bulk region is charge-free. Pioneering work in this area dates back to the 1960s, with notable contributions from G. I. Taylor and J. R. Melcher [8, 9], who investigated the deformation and stability of fluid-fluid interfaces under electric fields. The LDM was extended to model electrohydrodynamics of bio-membranes by treating the thin membrane as a zero-thickness interface with effective electric properties, e.g., capacitance C_m . Studies using this model have reported instabilities induced by various mechanisms, including ion currents across the membrane subjected to DC normal fields [10] and tangent fields [11], and capacitive current upon application of a DC field [12], and in AC fields with periods shorter than the capacitor charging time [13].

Although effective on a theoretical basis, the above studies neglect the thermal motion of the free charge. In a real system, the ions near an interface form a diffuse layer. This layer has a characteristic thickness, called the Debye screening length, which is typically few nanome-

ters. The Poisson-Nernst-Planck equation governs the dynamics of the charges within electrolytic materials, and it has been used extensively in electrokinetics to study membrane or fluid interfaces [14]. Ref. [15] investigated curvature-surface charge density coupling induced instabilities of the membrane, where the charges can flip to the other side and where they can diffuse on the same side, and [16] focused on such instability with strongly charged surfaces. [17, 18] analyzed the electrostatic correction to the surface tension bending rigidity on the instability with a finite-thickness membrane. [19, 20] proposed a zero-thickness model with Robin-type of boundary conditions, predicting electrokinetic corrections to the elastic moduli of the membrane, and a new destabilizing term in the growth rate of the membrane undulations due to ion current through the membrane. These studies report membrane instability arising from unbalanced electrical stress on the membrane, due to either surface charge [15, 16] or charge within the Debye layer [17–20]. Similar instabilities have also been observed in fluid-fluid interface systems, such as the velocity enhancement at electrolyte/liquid metal interfaces [21], and the perfect-dielectric liquid/electrolyte interfaces [22].

In a steady DC electric field normal to a non-conducting membrane, the LDM predicts that the fully-charged membrane capacitor suppresses instabilities [10]. Instability arises only in AC fields [13] or during the startup of a DC field [12], where the membrane acts as a short-circuited capacitor, leading to charge imbalances on its surfaces. However, the PNP model identifies a different mechanism, predicting instability even under steady-state DC fields due to negative tension in the membrane [19, 20]. The physical origin of this negative tension remains less intuitive, and we provide an explanation of the instability mechanism by examining charge redistribution within the Debye layer. Ref. [19, 20] focused on symmetric membranes, i.e. separating electrolyte solution with the same ions and concentrations. We extend the analysis to asymmetric electrolyte concentrations and demonstrate that such asymmetry has a stabilizing effect, mitigating the instability predicted by

the PNP model. This highlights the critical role of ionic distribution and membrane asymmetry in determining stability under electric fields. In Section II, we introduce the governing equations for two electrolyte layers of ions, separated by a thin ion-impermeable membrane. Section III discusses the base state solution and its linear stability. We further explore the effects of key parameters on instability in Section IV, identifying the sources of instability and elucidating why conductivity asymmetry reduces it. In addition, we show such asymmetric conductivity will result into the spontaneous curvature. Finally, conclusions and avenues for further research are summarized in Section V.

II. PROBLEM FORMULATION AND GOVERNING EQUATIONS

The system consists of two electrolyte solutions separated by a thin planar membrane impermeable to ions as shown in (Fig. 1). The concentrations of the positive and negative ions are n_i^+ and n_i^- , where $i = 1, 2$ refer to the upper fluid and the lower fluid, respectively. The electrodes are located at $z = \pm L$, where DC voltage of $2V$ is applied. The position of the flat membrane is $z = 0$. We consider the two electrolytes are both 1 : 1, with the same permittivity ε_f , but different concentration n_i^∞ . This implies a different conductivity of the electrolyte solutions, $\sigma_i = 2e^2\omega n_i^\infty$ [14], where ω is the mobility of ions and e is the elementary charge. We consider the membrane to be impermeable to ions.

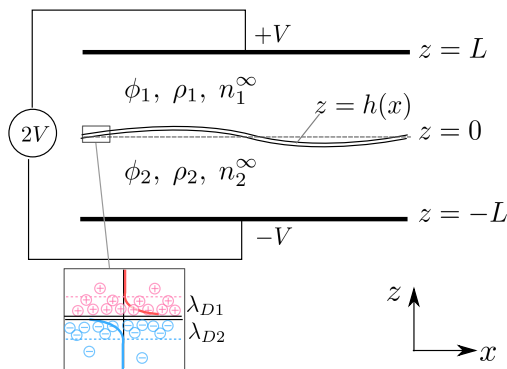


FIG. 1. A planar lipid bilayer membrane, with shape denoted by $z = h(x)$, separating electrolyte solutions with different concentration. The electrodes, with potential $\phi = \pm V$, are held at $z = \pm L$.

A. Governing equations

In the electrolyte, the governing equation for the electric potential ϕ is the Poisson's equation

$$\nabla^2 \phi_i = -\frac{\rho_i}{\varepsilon_f}, \quad (1)$$

where $\rho_i = e(n_i^+ - n_i^-)$ is the charge density, which obeys the linearized Poisson-Nernst-Planck equations

$$\frac{\partial \rho_i}{\partial t} + \mathbf{v}_i \cdot \nabla \rho_i = -\nabla \cdot \mathbf{j}_i, \quad (2a)$$

$$\mathbf{j}_i = -D \left(\nabla \rho_i + \frac{2e^2 n_i^\infty}{k_B T} \nabla \phi_i \right). \quad (2b)$$

The perturbations in the concentration $n_i^\pm = n_i^\infty + \delta n_i^\pm$ [20] are used to linearize the PNP, assuming small applied voltages compared to thermal voltage $k_B T/e$ [23]. The \mathbf{j}_i is the electric current density, $k_B T$ is the thermal energy, D is the ion diffusion coefficient (all ions are assumed to have the same mobility), and \mathbf{v}_i is the fluid velocity. Here we introduce the Debye length

$$\lambda_{D_i} = \left(\frac{2e^2 n_i^\infty}{\varepsilon_f k_B T} \right)^{-1/2} \quad (3)$$

that defines the characteristic length scale for charge relaxation in the electrolyte, and we define $\lambda_D = (\lambda_{D_1} \lambda_{D_2})^{1/2}$ as the composite Debye length in our asymmetric system, following the notation of [24].

In the context of biological membranes, inertia is negligible so that the velocity $\mathbf{v}_i = (u_i \hat{e}_x + v_i \hat{e}_z)$ and pressure p_i are solutions of the incompressible Stokes equations

$$-\nabla p_i + \mu_i \nabla^2 \mathbf{v}_i - \rho_i \nabla \phi_i = 0, \quad \nabla \cdot \mathbf{v}_i = 0, \quad (4)$$

where μ_i is the fluid viscosity and $-\rho_i \nabla \phi_i$ is the Coulomb body forces due to the electric field acting on the charge distributed in the bulk.

B. Boundary conditions

At the top and bottom electrodes $z = \pm L$, we impose the voltage $\phi_i(z = \pm L) = \pm V$, which neglects the polarization at the surface at electrodes [20] since we focus on the membrane dynamics. The distance between the electrodes is assumed to be much larger than the Debye length $L \gg \lambda_D$, such that the bulk electrolyte is neutral and charge density is negligible $\rho_i(z = \pm L) = 0$.

The membrane's position is represented by $z = h(x)$, with unit normal vector $\mathbf{n} = (-h_x, 1)/(1 + h_x^2)^{1/2}$ pointing upward. On the membrane, we apply a Robin-type boundary condition [19, 20]

$$\varepsilon_f \mathbf{n} \cdot \nabla \phi_i|_{z=h} = C_m V_m, \quad i = 1, 2, \quad (5)$$

where $V_m = \phi_1|_{z=h} - \phi_2|_{z=h}$ is the transmembrane potential, and $C_m = \varepsilon_m/d_0$ is the capacitance of the membrane with the thickness d_0 and permittivity ε_m . This BC was derived by mapping the continuity of the potential $\phi_i|_{z=h} = \phi_m|_{z=\pm d_0/2}$ and the continuity of the displacement field $\varepsilon_f \mathbf{n} \cdot \nabla \phi_i|_{z=h} = \varepsilon_m \mathbf{n} \cdot \nabla \phi_m|_{z=\pm d_0/2}$ to a zero-thickness membrane [19], where ϕ_m is the electric field inside the membrane and $i = 1(2)$ corresponding to $+(-)d_0/2$. The continuity of the displacement field

holds under the assumption of no adsorbed charges at the membrane interface. It is important to note that while the charge in the Debye layer at the membrane may be nonzero, the surface charge is zero. In fact, the net bulk charge integrated over the Debye layer in the electrokinetic model, expressed as $Q = \int_{\lambda_D} \rho dz$, corresponds to the surface charge in the leaky dielectric model. For a flat membrane, we can calculate the macroscopic charge according to Eq. (1):

$$Q_1 = \int_{z=h}^{z=+\infty} \rho_1 dz = \varepsilon_f \frac{\partial \phi_1}{\partial z} \Big|_{z=h} - \varepsilon_f \frac{\partial \phi_1}{\partial z} \Big|_{z=\infty} \approx \varepsilon_f \frac{\partial \phi_1}{\partial z} \Big|_{z=h}, \quad (6)$$

since $z = +\infty$ is taken as the position far from the membrane and electric field vanishes in the bulk $-\frac{\partial \phi_1}{\partial z} \Big|_{z=+\infty} = 0$. The macroscopic charge on the other side of the membrane, denoted as Q_2 , can be calculated similarly. Upon analysis, the Robin BC (5) further suggests $Q_1 = -Q_2$, signifying that the total charge on both sides of the membrane always remains balanced, regardless of conductivity.

Another interfacial condition is the non-flux condition [25]:

$$\mathbf{n} \cdot \mathbf{j}_1|_{z=h} = \mathbf{n} \cdot \mathbf{j}_2|_{z=h} = 0. \quad (7)$$

This indicates an insulating membrane, i.e., charge is not permitted to cross the membrane.

For the flow, the no-slip and no-penetration boundary condition applies for the velocity field at the electrodes $\mathbf{v}(z = \pm L) = \mathbf{0}$. The area-incompressibility of the membrane implies that the surface velocity is solenoidal, $\nabla_s \cdot \mathbf{v}_s = 0$, where $\nabla_s = (\mathbf{I} - \mathbf{n}\mathbf{n}) \cdot \nabla$ is the surface gradient operator. The normal stress balance on the interface is given by:

$$\llbracket \mathbf{n} \cdot \mathbf{T} \cdot \mathbf{n} \rrbracket_h = \mathbf{n} \cdot \boldsymbol{\tau}_m, \quad (8)$$

where we denote $\llbracket f \rrbracket_a = f_1(z = a) - f_2(z = a)$ as the jump of f at position $z = a$, and \mathbf{T} as the total stress consists with the hydrodynamic stress \mathbf{T}^{hd} and Maxwell's stress \mathbf{T}^{el}

$$\mathbf{T} = \underbrace{-p\mathbf{I} + \mu[\nabla\mathbf{v} + (\nabla\mathbf{v})^\top]}_{\mathbf{T}^{hd}} + \underbrace{\varepsilon_f[\mathbf{E}\mathbf{E} - (\mathbf{E} \cdot \mathbf{E})\mathbf{I}/2]}_{\mathbf{T}^{el}}. \quad (9)$$

The stresses jump across the membrane is balanced by membrane elastic stresses derived from the Helfrich energy [26]:

$$\boldsymbol{\tau}_m = -\kappa[(2H - C_0)(2H^2 - 2K_G + C_0H) + 2\nabla_s^2 H]\mathbf{n} + 2\Gamma H\mathbf{n} - \nabla_s \Gamma, \quad (10)$$

where H is the curvature, K_G is the Gaussian curvature, and Γ is the surface tension. C_0 is the bilayer spontaneous curvature arising from the asymmetry of the monolayers. In this stability study, we will initially neglect C_0

by assuming $C_0 d_0 \ll 1$ [27] for a membrane of zero thickness. We will address its effects in Sec. IV C.

Finally the kinematic condition determines the evolution of the interface:

$$v = \frac{\partial h}{\partial t} + u \frac{\partial h}{\partial x}. \quad (11)$$

C. Dimensionless parameters and rescaling

The parameters in the above equations are scaled using their characteristic values in the system:

$$\begin{aligned} \rho_i &\mapsto 2e\sqrt{n_1^\infty n_2^\infty} \rho_i, & \phi_i &\mapsto \frac{k_B T}{\underbrace{e}_{\phi_c}} \phi_i, & V &\mapsto \phi_c V, \\ (x, z) &\mapsto \lambda_D(x, z), & h &\mapsto \lambda_D h, & d_0 &= \lambda_D d, \\ t &\mapsto \underbrace{\frac{\mu \lambda_D^2}{\varepsilon_f \phi_c^2}}_{t_{el}} t, & p &\mapsto \frac{\mu}{t_c} p, \end{aligned} \quad (12)$$

where ϕ_c is the thermal voltage, and t_{el} is the time scale in electrohydrodynamic flow [10]. Using this time scale, the scaled PNP model is expressed as:

$$\alpha \left(\frac{\partial \rho_1}{\partial t} + \mathbf{v}_1 \cdot \nabla \rho_1 \right) = \nabla^2 \rho_1 + R^{1/2} \nabla^2 \phi_1, \quad (13a)$$

$$\nabla^2 \phi_1 = -\rho_1, \quad (13b)$$

where $R = \frac{\sigma_1}{\sigma_2} = \frac{n_1^\infty}{n_2^\infty}$ denotes the conductivity ratio. With $R \mapsto R^{-1}$, Eqs. (13) applies for phase 2. The α represents the time scale ratio between t_{el} and the characteristic charging time of the double-layer capacitor $t_c = \frac{\lambda_D L}{D}$ [23, 24]:

$$\alpha = \frac{\lambda_D^2}{D} \frac{1}{t_{el}} = \frac{1}{D} \frac{\varepsilon_f \phi_c^2}{\mu} = \frac{t_c}{t_{el}} \frac{\lambda_D}{L}. \quad (14)$$

In this study, we consider the situation where $\alpha \ll 1$, and set $\alpha = 0$. In this limit, the charge relaxation in Debye layer happens instantaneously, and the Debye layer remains at equilibrium when subjected to perturbations. The dimensionless Robin BC is given by

$$\mathbf{n} \cdot \nabla \phi_i|_{z=h} = \beta V_m|_{z=h}, \quad i = 1, 2, \quad (15)$$

where

$$\beta = \frac{C_m \lambda_D}{\varepsilon_f} = \frac{\varepsilon_m}{\varepsilon_f d} \quad (16)$$

is the dimensionless capacitance. The non-flux condition at the membrane remains the form in Eq. (7) with the dimensionless current

$$\mathbf{j}_1 = -\nabla(\rho_1 + \gamma^{-2} \phi_1), \quad \mathbf{j}_2 = -\nabla(\rho_2 + \gamma^2 \phi_2), \quad (17)$$

where we denote $\gamma = R^{-1/4}$ for convenience. The scaled Stokes equation is given by

$$-\nabla p + \nabla^2 \mathbf{v} - \rho \nabla \phi = 0. \quad (18)$$

The scaled normal stress balance on the interface is

$$\begin{aligned} & \llbracket -p + 2\partial_z v + \frac{1}{2}(\partial_z \phi)^2 - \frac{1}{2}\beta d(\partial_z \phi_m)^2 \rrbracket_{z=h} \\ & = -\frac{1}{Ca} [4H^3 - 4HK_G + 2\nabla_s^2 H - 2\bar{\Gamma}H], \end{aligned} \quad (19)$$

where the capillary number Ca compares the electric and bending stresses:

$$Ca = \frac{\lambda_D \varepsilon_f \phi_c^2}{\kappa}, \quad \bar{\Gamma} = \frac{\Gamma \lambda_D^2}{\kappa}. \quad (20)$$

The electric traction at the membrane consists of two parts, with $\llbracket \frac{1}{2}(\partial_z \phi)^2 \rrbracket$ coming from the electric field in the external medium, and $\llbracket -\frac{1}{2}\beta d(\partial_z \phi_m)^2 \rrbracket$ coming from the electric field $\mathbf{E}_m = -\nabla \phi_m$ in the membrane [28, 29]. We emphasize that although the Robin condition (15) effectively maps the electric field and charge density on both side of the membrane to a zero-thickness membrane, the ϕ_m term in Eq. (19) remains necessary to calculate the effective stress in the zero-thickness limit [17, 18, 20]. We will address it in Sec. III.

III. LINEAR STABILITY ANALYSIS

The membrane fluctuations impose small perturbation $h(x, t) = h_k e^{st+ikx}$ around a flat reference state. Any variable g is expanded in a series of the form $g = g^{(0)}(z, t) + g^{(1)}(z, x, t)$. The superscript (0) corresponds to the base state, and $g^{(1)} = g_k^{(1)} e^{st+ikx}$ is the first order solution due to the effect of the small undulations. For the convenience, we will drop the subscript k for the first order perturbation.

A. Base state

We consider the flat membrane as the base state, $h(x) = 0$, and the electric field is aligned in z direction, perpendicular to the membrane. For electrostatic fields, we solve Eq. (13a) and Eq. (13b), with the Robin BC (15) and non-flux condition (7) at the membrane, and $\rho_i(z \rightarrow \pm\infty) = 0$, $\phi_i(z \rightarrow \pm\infty) = \pm V$ at the far field, to obtain the charge distribution

$$\rho_1^{(0)} = \rho_m e^{-\frac{z}{\gamma}}, \quad \rho_2^{(0)} = -\gamma^2 \rho_m e^{\gamma z} \quad (21)$$

and the base state potential

$$\phi_1^{(0)} = -\gamma^2 \rho_m e^{-\frac{z}{\gamma}} + V, \quad \phi_2^{(0)} = \rho_m e^{\gamma z} - V, \quad (22)$$

where

$$\rho_m = \frac{2\beta V}{\gamma + (1 + \gamma^2)\beta} \quad (23)$$

is related to the jump in the charge density across the membrane, with $\llbracket \rho^{(0)} \rrbracket_{z=0} = (1 + \gamma^2)\rho_m$. Note that the base state current $\mathbf{j}_1^{(0)} = \mathbf{j}_2^{(0)} = \mathbf{0}$ for all z , not just at the membrane [24].

The base state field can be calculated as $\mathbf{E}_i^{(0)} = E_{z,i}^{(0)} \hat{e}_z = -\partial_z \phi_i^{(0)} \hat{e}_z$, which is non zero in the Debye layer. This represents a key difference from the base state field in LDM. In LDM, under the same physical setup, the base state field is zero unless there is ion current across the membrane [7, 10] or membrane capacitor is charging [12]. In our subsequent discussion, we will demonstrate the critical role played by the non-zero base state electric field $\mathbf{E}_i^{(0)}$ in the membrane instability. The transmembrane potential at base state is given by

$$V_m^{(0)} = \llbracket \phi^{(0)} \rrbracket_{z=0} = \frac{2V\gamma}{\gamma + (1 + \gamma^2)\beta}. \quad (24)$$

Correspondingly, the internal field $E_m^{(0)}$ is

$$E_m^{(0)} = -V_m^{(0)}/d = -\frac{\rho_m \gamma}{\beta d}, \quad (25)$$

where the constant internal field has been used due to the continuity of the potential at the membrane boundaries, which constitutes with $\varepsilon_m E_m^{(0)} = \varepsilon_f E_{z,i}^{(0)}|_{z=0}$ by substituting β in Eq. (16). The internal field $E_m^{(0)}$ is obtained by keeping a finite thickness d , and in Sec. III C we will show this field introduces negative tension and results into destabilization effect.

In the bulk fluid, the velocity is zero $\mathbf{v}_i^{(0)} = \mathbf{0}$, and the base-state pressure is obtained from the Stokes equation (18) as

$$p_i^{(0)} = \frac{1}{2} \left(\frac{\partial \phi_i^{(0)}}{\partial z} \right)^2 = \frac{1}{2} \gamma^2 \rho_m^2 e^{\mp 2z\gamma\mp 1} \quad (26)$$

by assuming $p_i^{(0)}(z \rightarrow \pm\infty) = 0$. This indicates that the pressure is continuous $\llbracket p^{(0)} \rrbracket_{z=0} = 0$ across the flat membrane.

B. Leading order equations

In the perturbed state, by setting $\alpha = 0$, the ion conservation and Poisson's equation become

$$(\partial_z^2 - k^2) (\rho_1^{(1)} + \gamma^{-2} \phi_1^{(1)}) = 0, \quad (27a)$$

$$(\partial_z^2 - k^2) (\rho_2^{(1)} + \gamma^2 \phi_2^{(1)}) = 0, \quad (27b)$$

$$(\partial_z^2 - k^2) \phi_i^{(1)} + \rho_i^{(1)} = 0, \quad (27c)$$

which can be solved by the first order potential

$$\phi_1^{(1)} = -\rho_m a_1 h e^{-l_1 z}, \quad \phi_2^{(1)} = -\rho_m a_2 h e^{l_2 z}, \quad (28)$$

and charge density

$$\rho_1^{(1)} = -\gamma^{-2}\phi_1^{(1)}, \quad \rho_2^{(1)} = -\gamma^2\phi_2^{(1)}. \quad (29)$$

The l_i represent the inverse characteristic length scale of the electrostatic potential near the slightly undulated membrane, with

$$l_1 = (\gamma^{-2} + k^2)^{1/2}, \quad l_2 = (\gamma^2 + k^2)^{1/2}. \quad (30)$$

The coefficients

$$a_1 = \left[\frac{(\gamma^2 + 1)\beta + l_2}{l_1 l_2 + \beta(l_1 + l_2)} \right], \quad a_2 = \left[\frac{(\gamma^2 + 1)\beta + \gamma^2 l_1}{l_1 l_2 + \beta(l_1 + l_2)} \right]. \quad (31)$$

can be obtained via imposing the first order of Robin BC at the membrane

$$\left(h\partial_{zz}\phi_i^{(0)} + \partial_z\phi_i^{(1)} \right)_{z=0} = \beta[\phi^{(1)} + h\partial_z\phi^{(0)}]_{z=0}, \quad (32)$$

Note that when subjected to perturbation, the first order current remains zero in both electrolytes $\mathbf{j}_1^{(1)} = \mathbf{j}_2^{(1)} = \mathbf{0}$.

To obtain the flow induced in the surrounding electrolyte due to the perturbation, we solve the first order incompressibility and the Stokes equation

$$\partial_z v_i^{(1)} + iku_i^{(1)} = 0, \quad (33a)$$

$$-\partial_z p_i^{(1)} + (\partial_z^2 - k^2)v_i^{(1)} - (\rho_i^{(1)}\partial_z\phi_i^{(0)} + \rho_i^{(0)}\partial_z\phi_i^{(1)}) = 0, \quad (33b)$$

$$-ikp_i^{(1)} + (\partial_z^2 - k^2)u_i^{(1)} - (ik\rho_i^{(0)}\phi_i^{(1)}) = 0. \quad (33c)$$

Rearranging Eqs. (33) gives rise to a fourth-order differential equation in v_i which is given by

$$(\partial_z^2 - k^2)^2 v^{(1)} = k^2(\phi^{(1)}\partial_z\rho^{(0)} - \rho^{(1)}\partial_z\phi^{(0)}) = 0. \quad (34)$$

By imposing $v_i(z \rightarrow \pm\infty) = 0$, we obtain the solution of the form $v_i^{(1)} = (B_i + C_i z)e^{\mp kz}$, where B_i and C_i are to be determined by appropriate boundary conditions in terms of perturbation variables. The continuity of the tangential velocity, together with the incompressibility of the interface at the first order impose $u_1^{(1)}|_{z=0} = u_2^{(1)}|_{z=0} = 0$. This reduces the kinetic equation to be simplify $v^{(1)} = \partial_t h = sh$, together with the continuity of the normal velocity we will have $v_1^{(1)}|_{z=0} = v_2^{(1)}|_{z=0} = sh$. These BCs determine the solutions as function of s, h . The pressure $p_i^{(1)} = (\partial_z^3/k^2 - \partial_z)v_i^{(1)} - (\rho^{(0)}\phi^{(1)})$ can be obtained as

$$p_1^{(1)} = 2ksh e^{-kz} - \rho_1^{(0)}\phi_1^{(1)}, \quad p_2^{(1)} = -2ksh e^{kz} - \rho_2^{(0)}\phi_2^{(1)}. \quad (35)$$

To determine the growth rate s , we need the normal traction balance at the interface

$$\left[h\partial_z \left[-p^{(0)} + \frac{1}{2}(\partial_z\phi^{(0)})^2 \right] - p^{(1)} + 2\partial_z v^{(1)} + \partial_z\phi^{(0)}\partial_z\phi^{(1)} - \beta d\partial_z\phi_m^{(0)}\partial_z\phi_m^{(1)} \right]_{z=0} = \frac{2}{Ca}(\bar{\Gamma}k^2 + k^4)h. \quad (36)$$

The term $h\partial_z [-p^{(0)} + \frac{1}{2}(\partial_z\phi^{(0)})^2]$ vanishes due to the stress balance at the base state, and $\partial_z v^{(1)} = 0$ due to the incompressibility of the membrane and the bulk fluids. From Eq. (36) we see three sources of electrostatic contribution to the membrane instability, i.e., one from the pressure difference $[-p]$ due to the body force, one from the external normal traction $[\partial_z\phi^{(0)}\partial_z\phi^{(1)}]$, and one from the internal normal traction $[-\partial_z\phi_m^{(0)}\partial_z\phi_m^{(1)}]$ of the membrane. Note that while the base state field $-\partial_z\phi_m^{(0)}$ is constant, the first order field $-\partial_z\phi_m^{(1)}$ varies across the membrane (see Appendix A and [20] for detailed calculation). For a zero-thickness model, this internal traction is needed to correct the electrohydrodynamic effect as seen in [20] and [18].

C. Linear growth rate

The growth rate can be determined from Eq. (36) as

$$4s = s_{\text{ex}} + s_{\text{in}} - \frac{2}{Ca}(\bar{\Gamma}k + k^3), \quad (37)$$

where s_{ex} represents the external contribution to the growth rate, including both body forces and normal traction, whereas the internal contribution s_{in} arises solely from normal traction:

$$s_{\text{ex}} = \frac{\rho_m^2}{k} \left[\underbrace{-(\gamma^2 a_2 + a_1)}_{\text{external body force}} + \underbrace{\gamma(\gamma^2 + 1)}_{\text{external normal traction}} \right], \quad (38a)$$

$$s_{\text{in}} = \frac{\rho_m^2 \gamma^2}{\beta} \left[2 - \frac{\beta d}{\gamma}(2\gamma - a_1 - a_2) \right] \frac{e^{kd} - 1}{(e^{kd} + 1)d}. \quad (38b)$$

The three components, along with the full growth rate in Eq. (37) is shown in Fig. 2. Note that in the zero thickness limit $d \rightarrow 0$, the internal normal traction term in Eq. (38b) reduces to

$$\lim_{d \rightarrow 0} s_{\text{in}} = \frac{\rho_m^2 \gamma^2}{\beta} k, \quad (39)$$

contributing linearly to the growth rate. This term is in agreement with [7] in the LDM framework.

Next, we examine the effect of each terms in the long-wave limit $k \rightarrow 0$. With a finite thickness d , the internal normal traction can be expanded as

$$\lim_{k \rightarrow 0} s_{\text{in}} = \frac{\rho_m^2}{\beta} \left[\gamma^2 k - \left(\frac{d}{2}\beta\gamma m_2 + \frac{d^2}{12}\gamma^2 \right) k^3 \right] + O(k^5), \quad (40)$$

with $m_2 = \gamma + (\gamma^2 - 1)^2 / [2(\beta\gamma^2 + \beta + \gamma)]$.

The body force in Eq. (38a) can be expand as

$$-(\gamma^2 a_2 + a_1) = -\gamma(\gamma^2 + 1) + s_2 k^2 - s_4 k^4 + O(k^6), \quad (41)$$

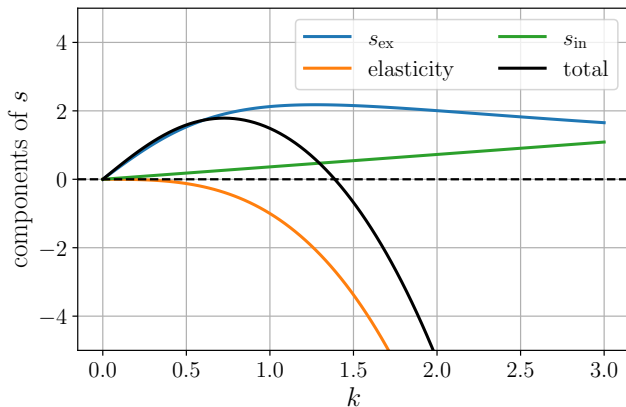


FIG. 2. The components of growth rate in Eq. (37) varying as a function of perturbation wavenumber k , with the “total” representing the full result as the sum of the external, internal, and elastic contributions. We consider symmetric conductivity with $\gamma = 1$, $V = 2$, $\beta = 10$, $Ca = 2$, $\bar{\Gamma} = 0$ and $d = 0$.

with

$$s_2 = \frac{\gamma(\gamma^2 + 1)}{2},$$

$$s_4 = \frac{\gamma^2 + 1}{8\gamma} \left(\gamma^4 + \gamma^2 + 1 + \frac{2\gamma(\gamma^2 - 1)^2}{\beta\gamma^2 + \beta + \gamma} \right).$$

Note that the constant term $-\gamma(\gamma^2 + 1)$ in Eq. (41) is canceled by the external normal traction in Eq. (38a), and the higher-order terms of k is left as the amount that the external normal traction exceeds the body force.

Thus, in the long-wave limit the growth rate has the form

$$4s = - \left(\frac{2}{Ca} \bar{\Gamma} - \rho_m^2 s_2 - \rho_m^2 \frac{\gamma^2}{\beta} \right) k - \left[\frac{2}{Ca} + \rho_m^2 s_4 + \frac{\rho_m^2 \gamma^2}{\beta} \left(\frac{d^2}{12} + \frac{m_2}{2\gamma} \beta d \right) \right] k^3. \quad (43)$$

The electrostatic contributions from the external $\rho_m^2 s_2 > 0$ and the internal $\rho_m^2 \frac{\gamma^2}{\beta} > 0$ destabilize the system, serving as negative corrections to the surface tension in the linear relation with k . The internal contribution is known as the Lippmann tension [30]. For the cubic contribution, the external term $\rho_m^2 s_4 > 0$ and the internal term $\frac{\rho_m^2 \gamma^2}{\beta} \left(\frac{d^2}{12} + \frac{m_2}{2\gamma} \beta d \right) > 0$ enhance the stabilizing effect of the bending modulus at shorter wavelength. When the conductivity is symmetric on both sides, i.e. $\gamma = 1$, we can reproduce the growth rate in [20], and the electrostatic corrections to the tension and bending modulus in [18, 29]. Such linear destabilizing effect is also reported in [15] as a consequence of the surface charge discrepancy between the two lipid layers for a no-tension membrane.

The instability observed in the present system, as reported by current studies and [20], appears to be inde-

pendent of ion current or transient effects. This presents a significant departure from the behavior predicted by the LDM model in [10], where, under identical conditions, the fully charged membrane remains stable. The disparity in stability predictions stemming from the same physical setup prompts the question: what underlying physical mechanisms govern this discrepancy? We will discuss the difference and elucidate the factors influencing stability in next section.

IV. INSTANTANEOUS CHARGE RELAXATION WITH ASYMMETRIC MEMBRANE

In this section, we will first examine the effects of key parameters, followed by a discussion on stabilizing electrostatic body forces and destabilizing electrostatic surface traction separately. Next, we will show the spontaneous curvature induced by the asymmetric conductivity. By the end, we will compare the linear stability analysis based on LDM and EK framework.

We consider the physical system with cells or giant lipid vesicles, and thus the fluids are aqueous salt solutions or water. Our analysis focuses on the case of equal-density and equal-viscosity fluids, $\rho_1 = \rho_2$ and $\mu_1 = \mu_2 \approx 10^{-3}$ Pa s. The value of the Debye length varies from $\lambda_D \sim 1 \mu\text{m}$ for pure water to $\lambda_D \sim 10 \text{ nm}$ for 1 mM NaCl. For pure water, the absolute permittivity is around $\epsilon_f \approx 7 \times 10^{-10}$ F m $^{-1}$. The diffusion coefficient is around $D \sim 10^{-9}$ m 2 s $^{-1}$. The character length scale for the gap between the electrodes is $L \sim 100 \mu\text{m}$. For the lipid membrane, typical values for the thickness is around $d_0 \sim 5 \text{ nm}$, and the capacitance is around $C_m \sim 0.01$ F m $^{-2}$. The elastic behavior is generally characterized by the bending modulus around $\kappa \sim 10^{-20}$ J. The typical value for the stretching modulus of a lipid membrane is around $\Gamma \sim 0.2$ J m $^{-2}$ [7], and the electric field has extra effects on it, such as the compressive electric stress effectively decreasing the isotropic tension [20, 31]. In this study we focus on the case of a freely floating membrane, which is tensionless in its base state $\Gamma = 0$. From these typical values we can obtain other dimensionless numbers as $Ca \sim 0.1 - 10$ and $\beta \sim 0.1 - 10$. The time scale ratio is around $\alpha \sim 0.1$, and we will consider the instantaneous charge relaxation, i.e. $\alpha = 0$ in this work. The conductivity ratio R can vary over a broad range [10].

A. Parameters effects

The growth rate in the long-wave limit Eq. (43), i.e. $k \rightarrow 0$, shows the electrostatic forces serves as the correction to the surface tension and bending modulus, which destabilize the system at the leading order, i.e. linear to k . The perturbation with smaller wavelength, greater k , will be dominated by the stabilizing effect of the elasticity. Thus, the system is unstable to a finite window

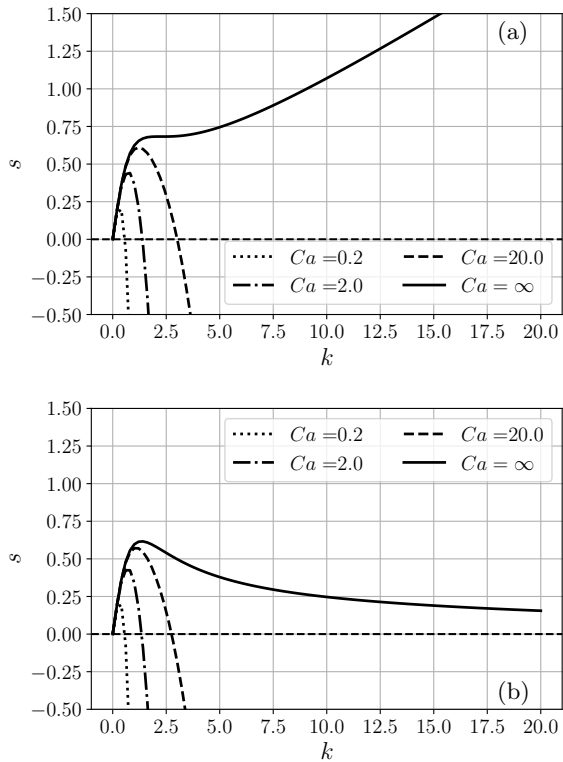


FIG. 3. The effect of Ca on growth rate s as a function of perturbation wavenumber k . We consider symmetric conductivity with $\gamma = 1$, $V = 2$, $\beta = 10$ for (a) $d = 0$ and (b) $d = 0.1$.

of wavenumbers $0 < k < k_c$, where k_c is the critical wavenumber corresponding to the marginal stable state $s = 0$ as the root of Eq. (37).

The effect of Ca is shown in Fig. 3. The growth rate monotonically increases with Ca . As $Ca \rightarrow +\infty$, the elasticity effect vanishes and all wavelengths are unstable due to the electrostatic forces. In the zero-thickness limit, the growth rate at larger k is dominated by the linear behavior of the internal normal traction for $Ca \rightarrow +\infty$, while for a finite thickness membrane, the the growth rate first increases then saturates to zero for $Ca \rightarrow +\infty$, which is similar to the description in LDM [10]. However, it is noteworthy that the length scale in this work is the Debye length, and thus $k \rightarrow \infty$ represents the perturbation with wavelength much smaller than Debye length, which differs from [10], where short-wave limit $k \rightarrow \infty$ is scaled with the inverse geometric length.

It is interesting to notice that the effect of β in Fig. 4(a) on the growth rate, is very similar to that of the conductivity of the membrane, g_m in [10], Fig. 2(a), where $g_m = G_m L / \sigma$ and G_m is the dimensional membrane conductivity. At β (g_m) = 0, the system is stable for all wavenumbers, while at β (g_m) $\rightarrow +\infty$ the growth rate saturates. Mathematically, such similar behavior can be understood from the continuous current condition at the

membrane for steady state in [10] (see Eq. (2.2)):

$$\mathbf{n} \cdot \mathbf{E}_i = g_m V_m, \quad i = 1, 2, \quad (44)$$

which is in the same form as the Robin condition (15) at the membrane: $\mathbf{n} \cdot (-\mathbf{E}_i) = \beta V_m$, where $\beta = C_m \lambda_D / \varepsilon_f$. The difference on sign of the electric field, i.e. $-\mathbf{E}_i$ is due to different relative direction of surface normal \mathbf{n} w.r.t. the potential at electrodes. Moreover, at these two limits, the internal normal stress is zero, and the system in current work has the same stress boundary at the membrane as in [10]. Thus, even if the dimensionless number g_m and β has very different physical meaning, and the membrane boundary condition Eq. (15) and Eq. (44) represents balance of the charge near membrane and continuity of the current separately, they do have the similar effect on the stability of the fully charged membrane mathematically.

Next, we will illustrate the physical meaning at two limits $\beta \rightarrow 0, +\infty$. As $\beta \rightarrow 0$, there is no charge accumulated in the Debye layer, i.e., the Debye layer vanishes. The base state potential are constant in space as $\phi_i^{(0)}(z) = \pm V$, and the electric field $E_{i,z}^{(0)}(z) = 0$. Thus, at this limit, the EK system behave like a LDM: without ion current ($g_m = 0$), the membrane will be stable. Increasing β represents increasing the effect of the membrane capacitance C_m , i.e. the ability to store charge at unite potential (Q_m/V_m), with $Q_m = |Q_i|$ (according to Eq. 6) as the macroscopic charge along the membrane on one side. As $\beta \rightarrow +\infty$, $V_m = 0$, and the Q_m also reaches its maximum as $\gamma \rho_m$, with $\rho_m|_{\beta \rightarrow +\infty} = 2V/(1 + \gamma^2)$. The membrane capacitance $C_m = \varepsilon_m/d_0 \rightarrow +\infty$ can be achieved by consider a membrane with zero-thickness $d_0 \rightarrow 0$ but with finite ε_m . From an electrical standpoint, the membrane acts as a simple fluid–fluid interface: without potential jump across the membrane, the Debye layers on both sides still stores charges, and the internal normal traction from internal membrane disappear $\rho_m^2 \gamma^2 / \beta|_{\beta \rightarrow 0} = 0$. In this limit, the Robin BCs in Eq. (15) reduces to the continuity of potential $[\phi] = 0$, and the continuity of the displacement field $[\varepsilon_f \mathbf{n} \cdot \mathbf{E}] = 0$ at the interface. These two boundary conditions was used in an EK model for the simple fluid interface [22] that is impermeable to ions. It differs from the interfacial condition using ion conservation [25, 32]. Mechanically, the membrane is different from a simple interface, due to the surface-incompressibility resulting from the conservation of lipids. The limit at $g_m \rightarrow 0$ is also discussed in [10], which represents a short-circuited capacitor and the membrane acts as a simple fluid–fluid interface.

In [10], the growth rate monotonically increases with g_m and then saturates, while in current system, the growth rate first increases then decreases with β and saturates to constant. This is due to the combination effect of internal and external effects. When excluding the internal normal traction (blue curve in Fig. 4(a)), the growth rate behaves monotonically. In Fig. 4(b), the external contribution to the growth rate increases with β and saturates at a constant value, whereas the

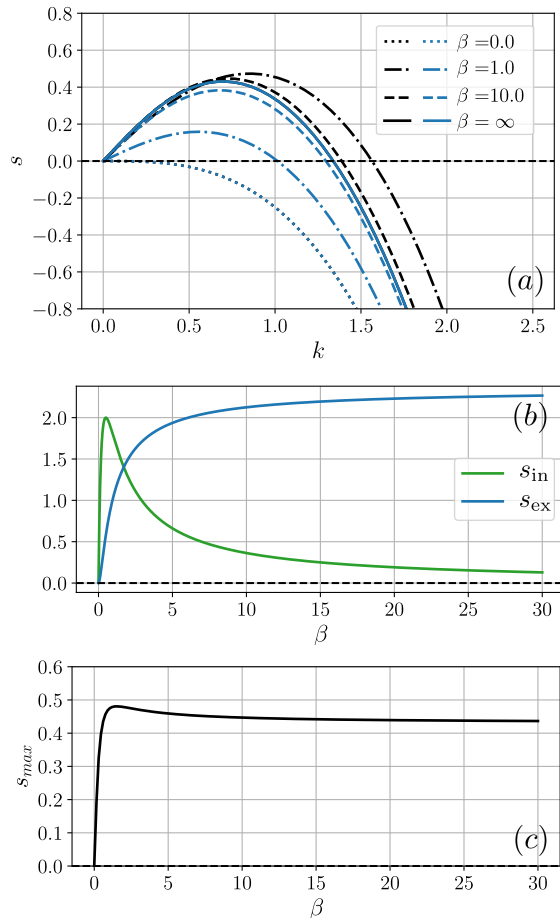


FIG. 4. (a) The effect of β on the growth rate, with black curve shows the full growth rate as in Eq. (37), while the blue curve excludes the contribution from the internal traction in Eq. (38b); (b) the effect of β on the external and internal contribution to the growth rate in Eq. (38) at $k = 1$; (c) the maximal (full) growth rate s_{max} as function of β . Note that the blue and black curve overlap at $\beta = 0, \infty$ in (a). We consider the system with parameters $V = 2$, $\gamma = 1$, $d = 0$, and $Ca = 2$.

internal traction contribution initially rises from zero at $\beta = 0$, peaks, and then decreases back to zero as $\beta \rightarrow \infty$. Specifically, $\lim_{\beta \rightarrow 0} s_{in} = \lim_{\beta \rightarrow \infty} s_{in} = 0$, corresponding to the overlap between the full growth rate (black curve) and the growth rate excluding internal traction (blue curve) at these limits in Fig. 4(a). The internal traction contribution reaches its maximum at $\beta = \frac{\gamma}{1+\gamma}$, with $\max s_{in} = \frac{V^2 \gamma^3}{1+\gamma}$. This peak results in the nonmonotonic behavior of the full growth rate in Fig. 4(a), which is further highlighted by the variation of the maximum growth rate shown in Fig. 4(c).

Fig. 5(a) shows the effect of the asymmetric conductivity γ on the growth rate. Due to the reversibility of the system, i.e. $s(\gamma) = s(1/\gamma)$, we only show results for $\gamma > 1$. It is very anti-intuition that the membrane subjected to the fluids with the symmetric conductiv-

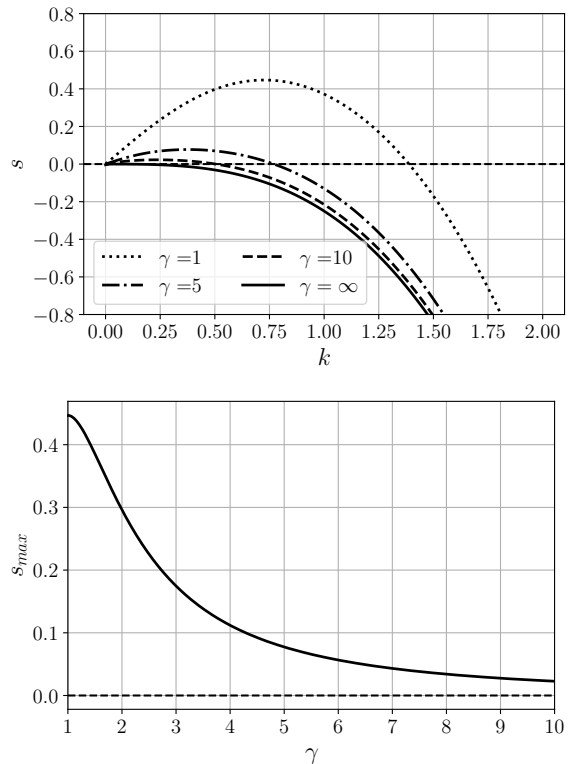


FIG. 5. (a) The effect of γ on growth rate s as a function of perturbation wavenumber k ; (b) maximal growth rate s_{max} as function of γ . We consider the system with $V = 2$, $\beta = 10$, and $Ca = 2$.

ity ($\gamma = 1$) undergoes the most intense instability. As γ increase from 1, the maximum growth rate decrease as shown in Fig. 5(b), and the window for the unstable wavenumbers get narrowed. As $\gamma \rightarrow +\infty$, the system become stable. This result is very different from the known literature [10], where the instability increase with the asymmetry of conductivity. To understand the cause of this difference, it is essential to first examine the mechanism of the instability and how it diverges from the LDM framework. This will be explored in detail in the remainder of this section.

B. Effect of electrostatic forces

1. Stabilizing electrostatic body forces

The Coulomb body forces in the Stokes equation (18), $\mathbf{f} = -\rho \nabla \phi$, tend to move the positive charges ρ in the direction of the electric field \mathbf{E} . In the base state, these body forces are balanced by the pressure gradient on both sides of the fluid, as evidenced by Eq. (26). Additionally, the flat interface remains free from normal traction arising from either electrostatic stress or elasticity, as well as surface tension.

To understand the stabilizing effect indicated in

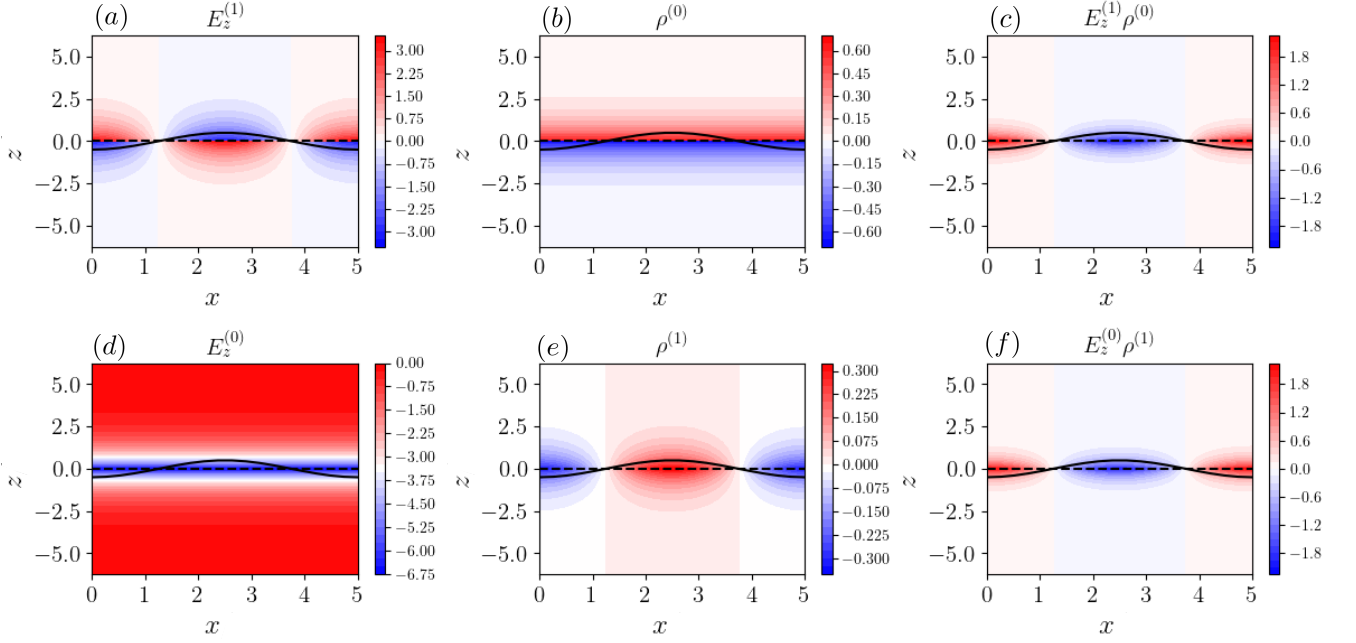


FIG. 6. z -component electric field E_z (a,d) and charge density ρ (b,e) for the base state and first order are used to illustrate the the first order body force component $\mathbf{f}^{(1)} \cdot \hat{e}_z = \rho^{(0)} E_z^{(1)} + \rho^{(1)} E_z^{(0)}$ in (c,f). We consider symmetric conductivity $\gamma = 1$, $\beta = 1$, $V = 1$.

Eq. (37) and Eq. (41), we illustrate the first order body force $\mathbf{f}^{(1)} = -(\rho^{(0)} \nabla \phi^{(1)} + \rho^{(1)} \nabla \phi^{(0)})$ in Fig. 6. The body force is calculated with a uni-modal perturbation with wavenumber $k = 0.2$, corresponding to a wavelength 5 times the Debye length, i.e., $x = 5$. The perturbation amplitude is set to $h = 0.5$. It is expected that the body force acts only on the fluid in the Debye layer, decaying exponentially in the bulk. Within the Debye layer, the body force points downward at the interface's crest and upward at the trough. This implies the restorative effect of the body force, consistent with the negative sign in the term Eq. (41) for small k .

2. Destabilizing external electrostatic surface traction

The external normal traction has the expression

$$\llbracket \partial_z \phi^{(0)} \partial_z \phi^{(1)} \rrbracket_{z=0} = (\partial_z \phi_1^{(0)} \partial_z \phi_1^{(1)} - \partial_z \phi_2^{(0)} \partial_z \phi_2^{(1)})|_{z=0}. \quad (45)$$

In LDM framework as in [10], when the membrane is fully charged, and no current cross the membrane, resulting in zero Ohmic current in the bulk fluid, the normal traction will be zero due to the absence of a base state electric field $\partial_z \phi_i^{(0)} = -E_z^{(0)} = 0$. In the current study, the base state electric field is nonzero at the membrane due to the Debye layer $\partial_z \phi_1^{(0)}|_{z=0} = \partial_z \phi_2^{(0)}|_{z=0} = \gamma \rho_m$. Thus,

Eq. (45) can be further simplified as

$$\begin{aligned} & \llbracket \partial_z \phi^{(0)} \partial_z \phi^{(1)} \rrbracket_{z=0} \\ &= \partial_z \phi_1^{(0)}|_{z=0} \llbracket \partial_z \phi^{(1)} \rrbracket_{z=0} = \partial_z \phi_1^{(0)} h \llbracket \rho^{(0)} \rrbracket_{z=0} \\ &= \underbrace{-\partial_z \phi_1^{(0)}}_{\text{base state field}} (-h) \underbrace{\rho_m (1 + \gamma^2)}_{\text{net charge density across membrane}} \end{aligned} \quad (46)$$

where $\llbracket \partial_z \phi^{(1)} \rrbracket_{z=0} = -h \llbracket \partial_{zz} \phi^{(0)} \rrbracket_{z=0} = h \llbracket \rho^{(0)} \rrbracket_{z=0}$ has been used according to the first order Robin BC (32). Consequently, we interpret the external electrostatic surface traction as the net force exerted on the fluid adjacent to the membrane, namely the net charge density $\llbracket \rho^{(0)} \rrbracket_{z=0}$ moving in the direction of the base state electric field $-\partial_z \phi_1^{(0)}$ (pointing downward), and modulated by the perturbed membrane at $(-h)$. After transforming from Fourier domain to physical domain, we found the traction have the same formulation but with $h = h(x)$. Then, when $h(x) < 0$, the surface traction will point downward and vice versa, which renders the membrane unstable to deformations. This implies the destabilizing effect of the external electrostatic normal traction, consistent with the positive sign in the term Eq. (37) for any small k .

In addition, we observe that in contrast to the LDM, the presence of a non-zero base state electric field $\mathbf{E}^{(0)}$ primarily contributes to the instability. In the LDM, a non-zero base state electric field necessitates either bulk current [7, 10] or membrane charging. However, within the EK framework, $\mathbf{E}^{(0)}$ consistently exists inde-

pendently of other effects due to the Debye layer. Intu-

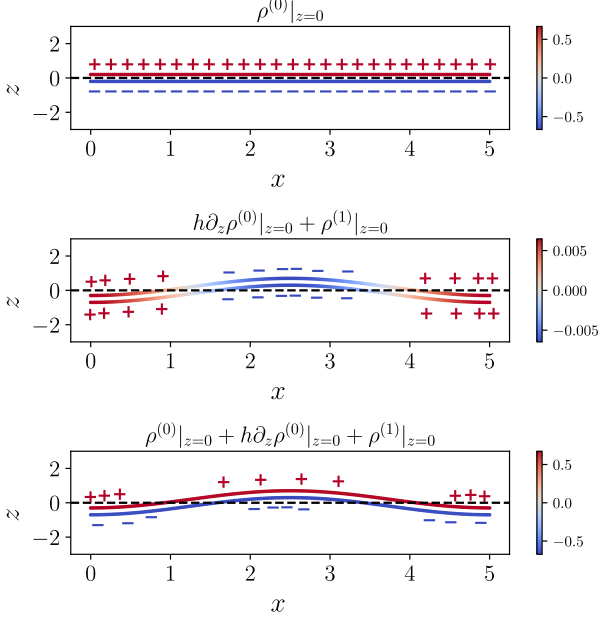


FIG. 7. The uniform charge density at the base state (a) redistributes due to the perturbation h . (b) shows the perturbed charge density at first order and (c) shows the total charge density at the membrane as the summation of plot (a) and (b). The figure shows the example with $\gamma = 1$, $\beta = 1$, $V = 1$.

itively, we can understand such instability through the charge redistribution. Fig. 7 shows the charge distribution in the fluid along the membrane. At the base state (Fig. 7(a)), the charge is uniformly distributed along the membrane. However, when subjected to a small perturbation (Fig. 7(b)), the linear correction causes positive charge accumulation at the troughs on both sides of membrane, while negative charge accumulates at the crests. As a result (Fig.7(c)), on the upper lipid, positive charge accumulates denser at the troughs compared to the crests, while on the lower lipid, negative charge accumulates less at the troughs than at the crests. This accumulation will further result in a force which tends to enhance the perturbation. Similar mechanics of the instability resulting from surface charge redistribution due to the membrane undulation are also discussed in [15]. Different from the present study, the surface charge in [15] are adsorbed on the interface, and such that compensates the charge distributed in Debye layer, i.e. each lipid layer is electroneutral.

Next, we aim to understand why the instability decreases with asymmetry of the conductivity. We consider the scenario where $\gamma \rightarrow 0$, i.e. $R = \frac{n_1^\infty}{n_2^\infty} \rightarrow \infty$. In this limit, $\rho_1^{(0)}|_{z=0} = \rho_m = \frac{2\beta V}{\gamma + (1+\gamma^2)\beta} \rightarrow 2V$, $\rho_2^{(0)}|_{z=0} = -\gamma^2\rho_m \rightarrow 0$, and the net charge density across membrane $[\rho^{(0)}]_{z=0} \rightarrow 2V$. However, the base state field

$\partial_z\phi_i^{(0)}|_{z=0} = \gamma\rho_m \rightarrow 0$, resulting in the entire external traction term approaching zero. Therefore, the instability decreases as $\gamma \rightarrow 0$. Similar results can be derived as $\gamma \rightarrow \infty$, where $[\rho^{(0)}]_{z=0} \rightarrow 2V$ and the base state field $\partial_z\phi_i|_{z=0} = \gamma\rho_m \rightarrow 0$. The result of these two limits is illustrated in Fig. 8, where the destabilizing external surface traction attains its maximum when subjected to the symmetric conductivity.

3. Destabilizing internal electrostatic surface traction

The electric stress induced by the rearranged charge at the membrane has also been used to explain the internal normal traction in [7], which establishes the system in the LDM framework, and the surface charge is brought to interface by the bulk current. In their work, the compressive electrostatic stress has the form $\varepsilon_m E_m^2/2$. For a perfectly flat membrane, the electric stress in the membrane is symmetrically balanced on both sides of the membrane. When subjected to a perturbation, the redistributed charge $\Sigma_\pm \sim \pm\varepsilon_m E_m$ results into an unbalanced stress $(\Sigma_+^2 - \Sigma_-^2)/\varepsilon_m$. This analysis shares the same situation as ours, where the the base state macroscopic charge is $Q_i^{(0)} = \pm E_z^{(0)}|_{z=0} = \pm\beta d E_m^{(0)}$.

In our work, the first-order internal traction has the form

$$-\left[\beta d \partial_z \phi_m^{(0)} \partial_z \phi_m^{(1)}\right]_{z=\pm d/2} = \beta d E_m^{(0)} \left[\partial_z \phi_m^{(1)}\right]_{z=\pm d/2} \quad (47)$$

where the jump of the first order internal field $\left[\partial_z \phi_m^{(1)}\right]_{z=\pm d/2} \sim E_m^{(0)} dk^2 h$ is nonzero due to the perturbation (see Appendix A for expression). Intuitively, we can understand this jump as the virtual charges inside the membrane, and driven by the field $E_m^{(0)}$. Like the external traction, we consider the deformation in physical domain, which has the same formulation but with $h = h(x)$. At the membrane where $h(x) < 0$, the virtual charges are positive and driven by a negative internal field. Thus, the internal surface traction will point downward and vice versa, which renders the membrane unstable to deformations.

As discussed around Eq. (37), the internal normal traction in this work is in agreement with the total traction in [7], where the external traction vanishes in the limit of large ε_m and small membrane conductivity σ_m . In their work, the internal field E_m is related with the external field E though the conservation of current, and thus $E_m \sim E\sigma_i\sigma_m$, and thus small σ_m indicates a large internal field. In our work, the internal field $E_m^{(0)} \sim E_z^{(0)}|_{z=0}/(\beta d)$, and thus $\beta d \ll 1$ indicates a large fields ratio $E_m^{(0)}/E_z|_{z=0}$. Keeping d finite and letting $\beta \rightarrow 0$, we see the destabilizing effect of the normal traction documented by the internal traction in Eq. (43). This conclusion is in agreement with [19, 29], where the ‘‘inside’’ contribution is in general dominant when large

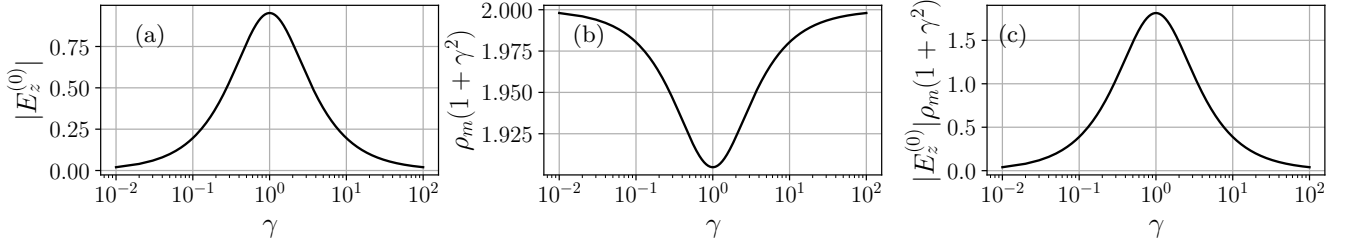


FIG. 8. The effect of the conductivity ratio γ on (a) base state electric field $E_z^{(0)}|_{z=0}$, (b) the base state charge density across the membrane, and (c) the external normal surface traction calculated according to Eq. (46). The example is given with $\beta = 10$, $V = 1$.

voltage drop occurs across the membrane, and in our work $\beta \rightarrow 0$ yields the largest transmembrane potential V_m .

Similar to the external surface traction, as $\gamma \rightarrow 0$ or $\gamma \rightarrow +\infty$, the base state external field $E_z^{(0)}|_{z=0} \rightarrow 0$ and thus $E_m^{(0)} \rightarrow 0$, and the interal traction term vanishes.

C. Spontaneous curvature

Biomimetic and biological membranes consist of two monolayers which are typically exposed to different environments and may differ in packing density of the lipid molecule's head and tail [33]. These asymmetry will result into the torque across the membrane and such that the membranes prefer to curve and characterized by the spontaneous curvature. In this study, the asymmetric conductivity of the electrolytes on both sides of the membrane changes the stress distribution, and we will examine the spontaneous curvature C_0 calculated as the first moment of the lateral stress tensor [18]. After scaling C_0 with λ_D^{-1} , we will have

$$C_0 = Ca \int_{-\infty}^{+\infty} T_{xx}^{(0)} z dz, \quad (48)$$

The component T_{xx} can be obtained as

$$T_{xx} = -p^{(0)} - \frac{1}{2} E_z^{(0)2} = -E_z^{(0)2}, \quad (49)$$

where the base state pressure $p^{(0)}$ in Eq. (26) can also be obtained from $T_{zz} = -p^{(0)} + \frac{1}{2} E_z^{(0)2} = 0$. Basing on this stress profile, the spontaneous curvature can be obtained as

$$\begin{aligned} C_0 &= Ca \int_{-\infty}^{+\infty} T_{xx}^{(0)} z dz = \frac{Ca\rho_m^2}{4} (1 - \gamma^4). \\ &= Ca\beta^2 V^2 \frac{1 - \gamma^4}{[\gamma + (1 + \gamma^2)\beta]^2}. \end{aligned} \quad (50)$$

If $\gamma = 1$, the spontaneous curvature vanishes in a symmetric system, and this corresponds to the result in [18]

for the finite-thickness membrane with zero charge density inside. However, the asymmetric conductivities of the bulk fluids tend to curve the flat membrane through the first moment of the stress. $\gamma > 1$ corresponds to the conductivity $\sigma_1 < \sigma_2$, and the membrane tends to have a negative curvature. The cell geometry alerted by the asymmetric electric double layers adjacent to the membrane is also reported in experimental work [34].

For current selecting of parameters, with $\beta = 10$, $V = 1$, $\gamma = 2$, $Ca = 2$, we will have $\rho_m \approx 0.4$, and $|C_0| \approx 0.6$. Also, C_0 increase with γ for $\gamma > 1$. As $\gamma \rightarrow +\infty$, $|C_0|_{\max} = CaV^2 = 2$. The $|C_0| \sim O(1)$ indicates that the spontaneous curvature is of the same scale as the inverse Debye length. Thus, in the zero-thickness membrane assumption, we will always have $|C_0|d \ll 1$, and it is valid to assume a flat membrane to conduct linear stability analysis.

D. Small perturbation assumption

The infinitesimal perturbation assumption serves as a fundamental principle in the linear stability analysis of membranes or interfaces, a concept employed in EK modeling as seen in our present study and [20], as well as in LDM, as demonstrated in [10]. However, it becomes important to examine the perturbation amplitude relative to the Debye length.

The LDM assumes electroneutrality of the bulk fluid and an infinitesimal amount of free charge confined to the interface. Consequently, the model is inherently constrained by the thin Debye layer limit. Linear analysis derived from the LDM overlooks any dynamic behavior within the Debye layer, implicitly assuming perturbation amplitudes surpassing the Debye layer's dimensions.

In the EK model, when expanding the leading-order variables from $z = h$ to $z = 0$, it becomes crucial to validate the linear approximation due to the anticipated abrupt change within the Debye layer. For instance, in the expansion of the Robin condition (15), we expand the base state electric field at the membrane as follows:

$$\partial_z \phi_i^{(0)}|_{z=h} \approx \partial_z \phi_i^{(0)}|_{z=0} + h \partial_{zz} \phi_i^{(0)}|_{z=0}, \quad (51)$$

by assuming h to be small. However, when considering

the exponential distribution of the base state potential $\phi_i^{(0)}$, we encounter $\partial_z \phi_2^{(0)} = Ae^{\gamma z}$. Substituting $z = h$ into $\partial_z \phi_2^{(0)}$, we find that to validate the expansion (51), i.e.

$$Ae^{\gamma h} \approx A(e^{\gamma 0} + h\gamma e^{\gamma 0}) = A(1 + \gamma h), \quad (52)$$

the condition $|\gamma h| \ll 1$ is necessary. Similarly, after applying the same procedure to the upper fluid $\partial_z \phi_1^{(0)}$, we derive the full constraint $|h| \ll \min(\gamma, \gamma^{-1})$ on the perturbation amplitude to ensure the validity of the linear stability analysis. In cases where the conductivity on both sides of the membrane is symmetric, i.e. $\gamma = 1$, and $|h| \ll 1$, we intuitively conclude that the linear analysis is only valid for perturbations smaller than the Debye layer.

Now the discrepancy between the linear analyses stemming from the EK and LDM frameworks become apparent. In the EK model, the initial perturbation is assumed to be smaller than the Debye layer ($h \ll 1 \ll L/\lambda_D$) and intensifies when exposed to instability induced by the electric field near the membrane. Conversely, the LDM presupposes perturbations larger than the Debye layer ($1 \ll h \ll L/\lambda_D$), with the thin Debye layer riding atop the deformed membrane, which gets stabilized when subjected to a zero electric field in the bulk. This inherent distinction naturally prompts a fundamental question: How can we systematically determine the growth rate that effectively bridges the gap between the EK and LDM approaches, thereby accurately predicting the stability of perturbations with arbitrary amplitudes?" One potential solution is to explore the dynamics beyond the linear regime within the EK framework. By doing so, we anticipate observing the system transitioning to the base state, or other equilibrium states, through different manifolds when subjected to a significant perturbation.

An accompanying question arises: what is the final state of the unstable membrane in the current study, given that the perturbation cannot grow indefinitely due to the conservation of lipid? We anticipate that nonlinearity will drive the system towards another equilibrium state, resulting in the emergence of stationary patterns in the membrane. For instance, [15] predicates a stable state with nonzero curvature as a consequence of the curvature–charge density coupling, where the transition from a flat membrane is induced when the Debye length is increased. This question can also be tackled by exploring nonlinearity, using methods such as fully nonlinear simulations or reduced nonlinear models like amplitude equations or long-wave equations as in [35]. Extending the EK framework to incorporate nonlinear dynamics will be the focus of our future work.

V. CONCLUSION AND OUTLOOK

The present work investigates the linear instability of a zero-thickness lipid membrane under a DC electric field,

subjected to fluids with asymmetric conductivity. An electrokinetic model with the Debye-Hückell approximation is adopted to capture the dynamics of diffuse layers formed near the membrane. The capacitive effect of the membrane is found to be critical for the onset of instability, due to which the charge accumulates inside the Debye layer. Upon perturbation, the charge redistributes and exerts a net force as surface traction on the fluid adjacent to the membrane, leading to system destabilization. While the electrostatic body force tends to stabilize the system, it is unable to counteract the normal traction. The asymmetric conductivity stabilizes the membrane by reducing the base state electric field. This prediction diverges from that of the LDM framework, which overlooks the dynamics of charge within the Debye layer.

The developed analysis is applicable only to perturbations smaller than the Debye layer. It is of interest to develop a model that systematically bridges the regimes of dimensional perturbation $h \ll \lambda_D$, $h \sim \lambda_D$ and $L \gg h \gg \lambda_D$. Such a model would be able to reconcile the contrasting stability predictions made by the present EK framework ($h \sim \lambda_D$) and the LDM framework ($L \gg h \gg \lambda_D$). One potential approach is to extend the current model into the nonlinear regime, allowing for illustration of the dynamical structure around the base state. Additionally, we anticipate that this nonlinear model will uncover other nontrivial equilibrium states, potentially revealing new patterns within the system.

Another intriguing factor to investigate is the non-equilibrium effect. The present study assumes instantaneous charge relaxation, and under this assumption, the Debye layer remains in equilibrium when subjected to perturbations. However, in dynamic conditions, the bulk conduction process is inherently unsteady and influenced by ion convection due to fluid motion accompanying membrane deformation. In other words, with finite α , the perturbation breaks the equilibrium state, causing charge in the bulk to move to or leave the Debye layer. This results in a transient current in the bulk that either charges or discharges the Debye layer. Such transient effects on stability have been studied in previous works [10, 12, 20], where these effects introduce new instabilities in the system. However, in the EK framework, [20] neglects the ion convection and considers a constant current through the bulk and membrane that is independent of the perturbation in the linear order. It would be of interest to include finite α in the current system and investigate how membrane deformation and ion convection modulate instability.

VI. ACKNOWLEDGMENTS

This research was supported by NIGMS award 1R01GM140461.

- [1] C. A. Jordan, E. Neumann, and A. E. Sowers, *Electroporation and electrofusion in cell biology* (Springer Science & Business Media, 1989).
- [2] J. C. Weaver and Y. A. Chizmadzhev, Theory of electroporation: a review, *Bioelectrochem. Bioenerg.* **41**, 135 (1996).
- [3] J. Teissie, M. Golzio, and M. Rols, Mechanisms of cell membrane electroporation: a minireview of our present (lack of?) knowledge, *Biochim. Biophys. Acta* **1724**, 270 (2005).
- [4] R. Dimova, N. Bezlyepkina, M. D. Jordö, R. L. Knorr, K. A. Riske, M. Staykova, P. M. Vlahovska, T. Yamamoto, P. Yang, and R. Lipowsky, Vesicles in electric fields: Some novel aspects of membrane behavior, *Soft Matter* **5**, 3201 (2009).
- [5] K. A. Riske and R. Dimova, Electro-deformation and poration of giant vesicles viewed with high temporal resolution, *Biophysical journal* **88**, 1143 (2005).
- [6] K. A. Riske and R. Dimova, Electric pulses induce cylindrical deformations on giant vesicles in salt solutions, *Biophysical journal* **91**, 1778 (2006).
- [7] P. Sens and H. Isambert, Undulation instability of lipid membranes under an electric field, *Phys. Rev. Lett.* **88**, 128102 (2002).
- [8] G. I. Taylor and A. D. McEwan, The stability of a horizontal fluid interface in a vertical electric field, *J. Fluid Mech.* **22**, 1–15 (1965).
- [9] E. B. Devitt and J. R. Melcher, Surface electrohydrodynamics with high-frequency fields, *Phys. Fluids* **8**, 1193 (1965).
- [10] J. Seiwert, M. J. Miksis, and P. M. Vlahovska, Stability of biomimetic membranes in dc electric fields, *J. Fluid Mech.* **706**, 58–70 (2012).
- [11] Y.-N. Young, S. Veerapaneni, and M. J. Miksis, Long-wave dynamics of an inextensible planar membrane in an electric field, *Journal of fluid mechanics* **751**, 406 (2014).
- [12] J. T. Schwalbe, P. M. Vlahovska, and M. J. Miksis, Lipid membrane instability driven by capacitive charging, *Phys. Fluids* **23**, 041701 (2011).
- [13] J. Seiwert and P. M. Vlahovska, Instability of a fluctuating membrane driven by an ac electric field, *Phys. Rev. E* **87**, 022713 (2013).
- [14] D. A. Saville, Electrohydrodynamics: the taylor-melcher leaky dielectric model, *Annu. Rev. Fluid Mech.* **29**, 27 (1997).
- [15] V. Kumaran, Instabilities due to charge-density-curvature coupling in charged membranes, *Phys. Rev. Lett.* **85**, 4996 (2000).
- [16] V. Kumaran, Effect of surface charges on the curvature moduli of a membrane, *Phys. Rev. E* **64**, 051922 (2001).
- [17] T. Ambjörnsson, M. A. Lomholt, and P. L. Hansen, Applying a potential across a biomembrane: Electrostatic contribution to the bending rigidity and membrane instability, *Phys. Rev. E* **75**, 051916 (2007).
- [18] B. Loubet, P. L. Hansen, and M. A. Lomholt, Electromechanics of a membrane with spatially distributed fixed charges: Flexoelectricity and elastic parameters, *Phys. Rev. E* **88**, 062715 (2013).
- [19] D. Lacoste, G. I. Menon, M. Z. Bazant, and J. F. Joanny, Electrostatic and electrokinetic contributions to the elastic moduli of a driven membrane, *Eur. Phys. J. E* **28**, 243 (2009).
- [20] F. Ziebert, M. Z. Bazant, and D. Lacoste, Effective zero-thickness model for a conductive membrane driven by an electric field, *Phys. Rev. E* **81**, 031912 (2010).
- [21] A. J. Pascall and T. M. Squires, Electrokinetics at liquid/liquid interfaces, *J. Fluid Mech.* **684**, 163–191 (2011).
- [22] P. Gambhire and R. Thakkar, Electrokinetic model for electric-field-induced interfacial instabilities, *Phys. Rev. E* **89**, 032409 (2014).
- [23] M. Z. Bazant, K. Thornton, and A. Ajdari, Diffuse-charge dynamics in electrochemical systems, *Phys. Rev. E* **70**, 021506 (2004).
- [24] S. Zhao, B. Balu, Z. Yu, M. J. Miksis, and P. M. Vlahovska, Diffuse-charge dynamics across a capacitive interface in a dc electric field (2025), arXiv:2502.11319 [cond-mat.soft].
- [25] Y. Mori and Y.-N. Young, From electrodiffusion theory to the electrohydrodynamics of leaky dielectrics through the weak electrolyte limit, *J. Fluid Mech.* **855**, 67 (2018).
- [26] U. Seifert, Fluid membranes in hydrodynamic flow fields: Formalism and an application to fluctuating quasispherical vesicles in shear flow, *Eur. Phys. J. B* **8**, 405 (1999).
- [27] U. Seifert and S. A. Langer, Viscous modes of fluid bilayer membranes, *Europhys. Lett.* **23**, 71 (1993).
- [28] H. Isambert, Understanding the electroporation of cells and artificial bilayer membranes, *Phys. Rev. Lett.* **80**, 3404 (1998).
- [29] D. Lacoste, M. C. Lagomarsino, and J. Joanny, Fluctuations of a driven membrane in an electrolyte, *Europhys. Lett.* **77**, 18006 (2007).
- [30] P.-C. Zhang, A. M. Keleshian, and F. Sachs, Voltage-induced membrane movement, *Nature* **413**, 428 (2001).
- [31] D. Needham and R. Hochmuth, Electro-mechanical permeabilization of lipid vesicles. role of membrane tension and compressibility, *Biophys. J.* **55**, 1001 (1989).
- [32] O. Schnitzer and E. Yariv, The taylor-melcher leaky dielectric model as a macroscale electrokinetic description, *J. Fluid Mech.* **773**, 1–33 (2015).
- [33] H.-G. Döbereiner, Properties of giant vesicles, *Curr. Opin. Colloid Interface Sci.* **5**, 256 (2000).
- [34] H. A. Faizi, R. Dimova, and P. M. Vlahovska, Electromechanical characterization of biomimetic membranes using electrodeformation of vesicles, *Electrophoresis* **42**, 2027 (2021).
- [35] Y.-N. Young and M. J. Miksis, Electrohydrodynamic instability of a capacitive elastic membrane, *Physics of Fluids* **27**, 022102 (2015).

Appendix A: Calculation of internal normal traction

The perturbed internal potential inside the membrane $z < |d/2|$ are governed by Laplace's equation

$$(\partial_z^2 - k^2)\phi_m^{(1)} = 0, \quad (\text{A1})$$

since there is no charge inside. The first-order internal potential can be solved as

$$\begin{aligned} \phi_m^{(1)} = \frac{e^{\frac{dk}{2}}}{e^{2dk} - 1} & \left[\left(\phi_m^{(1)}|_{z=d/2} e^{dk} - \phi_m^{(1)}|_{z=-d/2} \right) e^{kz} \right. \\ & \left. + \left(\phi_m^{(1)}|_{z=d/2} e^{dk} - \phi_m^{(1)}|_{z=-d/2} \right) e^{-kz} \right]. \quad (\text{A2}) \end{aligned}$$

The $\phi_m^{(1)}$ at the membrane can be evaluated through the expansion of continuity of the potential

$$\begin{aligned} \phi_m^{(1)}|_{z=d/2} = \phi_1^{(1)}|_{z=d/2} + \left(\frac{\partial \phi_1^{(0)}}{\partial z}|_{z=d/2} - \frac{\partial \phi_m^{(0)}}{\partial z}|_{z=d/2} \right) h \\ \approx [E_m^{(0)} + \rho_m(\gamma - a_1)]h, \quad (\text{A3a}) \end{aligned}$$

$$\begin{aligned} \phi_m^{(1)}|_{z=-d/2} = \phi_2^{(1)}|_{z=-d/2} + \left(\frac{\partial \phi_2^{(0)}}{\partial z}|_{z=-d/2} - \frac{\partial \phi_m^{(0)}}{\partial z}|_{z=-d/2} \right) h \\ \approx [E_m^{(0)} + \rho_m(\gamma - a_2)]h, \quad (\text{A3b}) \end{aligned}$$

where external potential and field at the membrane are approximated using values at $z = 0$. After substituting Eq. (A3) into Eq. (A2), the internal normal stress can be

obtained as

$$\begin{aligned} \left[\frac{\varepsilon_m}{\varepsilon_f} \partial_z \phi_m^{(0)} \partial_z \phi_m^{(1)} \right]_{z=\pm d/2} &= \frac{\varepsilon_m}{\varepsilon_f} \partial_z \phi_m^{(0)} \left[\partial_z \phi_m^{(1)} \right]_{z=\pm d/2} \\ &= \beta d (-E_m^{(0)}) [2E_m^{(0)} + \rho_m(2\gamma - a_1 - a_2)] \frac{k(e^{dk} - 1)}{e^{dk} + 1} h \\ &= -\frac{\rho_m^2 \gamma^2}{\beta} \left[2 - \frac{\beta d}{\gamma} (2\gamma - a_1 - a_2) \right] \frac{k(e^{kd} - 1)}{(e^{kd} + 1)d} h \quad (\text{A4}) \end{aligned}$$

by substituting $E_m^{(0)} = -\rho_m \gamma / (\beta d)$.

In the limit $d \rightarrow 0$, the term $\frac{k(e^{kd} - 1)}{(e^{kd} + 1)d} \rightarrow k^2/2$.

With d finite, and in the limit $k \rightarrow 0$, we can evaluate

$$\begin{aligned} (2\gamma - a_1 - a_2) &= \left[\gamma + \frac{(\gamma^2 - 1)^2}{2(\beta\gamma^2 + \beta + \gamma)} \right] k^2 + O(k^4), \\ \frac{k(e^{kd} - 1)}{(e^{kd} + 1)d} &= \frac{1}{2} \left(k^2 - \frac{d^2}{12} k^4 \right) + O(k^6), \end{aligned}$$

and these terms are used to evaluate the growth rate at long-wave limit.